Rheol Acta (2005) 45: 132–141
DOI 10.1007/s00397-005-0002-1

ORIGINAL CONTRIBUTION

Alireza S. Sarvestani
Catalin R. Picu

A frictional molecular model for the viscoelasticity of entangled polymer nanocomposites

Received: 24 November 2004
Accepted: 14 April 2005
Published online: 22 July 2005

A. S. Sarvestani · C. R. Picu (✉)
Department of Mechanical,
Aerospace and Nuclear Engineering,
Rensselaer Polytechnic Institute,
Troy, NY 12180, USA
E-mail: picuc@rpi.edu
Tel.: +1-518-2762195
Fax: +1-518-2766025

Abstract The dynamics of polymer melts and concentrated solutions reinforced with nanoscale rigid spherical particles is analyzed. Nanocomposites with low filler volume fraction and strong polymer-filler interactions are considered. Entanglement effects are represented by requiring the diffusion in the chain contour direction to be more pronounced than in the direction transverse to the chain primitive path. Filler particles are treated as material points. They reduce the polymer mobility in both longitudinal and transverse tube directions due to short-range energetic filler-polymer interactions. Hence, the contribution to chain dynamics and stress production of both filler-polymer and polymer-polymer interactions is considered to be purely frictional in nature. In the model, the strain rate sensitivity is associated with the thermal motion of chains, with the convective relaxation of entanglement constrains and with the polymer-filler attachment/detachment process. The effect of model parameters is discussed and the predictions are compared with experimental data.

Keywords Polymer nanocomposites · Topological and energetic constraint release

Introduction

Experimental observations indicate substantial differences in the rheology and dynamics of polymer liquids reinforced with colloidal and nanosize particles compared to complex fluids filled with micron sized particles (Reynaud et al. 2001; Zhang and Archer 2002, 2004; Donnet 2003). The filler size effect on the overall material behavior has been attributed to either inter-particle or polymer-particle energetic interactions, both occurring at the nanoscale. The first mechanism originates from the formation of spatial agglomerated structures of small particles (due to electrostatic and van der Waals' forces) and the evolution of these structures during loading (Leonov 1990; Heinrich and Klüppel 2002; Cassagnau and Mélis 2003). When fillers are well dispersed in the matrix, reducing the filler size while preserving the filler volume fraction leads to a dramatic increase of interfacial area and a reduction of the average wall-to-wall distance between fillers. Under such circumstances, a large fraction of chains are in contact with at least one filler, some of them forming bridges between neighboring particles. Very similar to the rheology of confined polymer thin films (Subbotin et al. 1995), the dynamics of such systems is controlled by the polymer-filler affinity and the stick-slip motion of chains close to the filler surface (Havet and Isayev 2001, 2003). This perturbs the viscoelastic behavior of the entire matrix phase. Such an effect also exists in composites with much larger fillers (e.g. micron size); however, the volume of perturbed matrix is limited to the interfacial boundary layer which represents a negligible fraction of the total volume of the material.

Classical homogenization methods developed for composites containing large fillers (much larger than the chain size) do not capture size effects associated with the filler dimensions. In these formulations, the overall viscoelastic properties are predicted in terms of the filler volume fraction only. In order to predict the behavior of nanocomposites with non-agglomerated fillers, the effective viscoelastic properties of this new *perturbed* polymer matrix must be determined. Along these lines, we recently proposed such a model based on the theory of transient networks (Sarvestani and Picu 2004). This formulation applies to nanofilled polymeric mixtures in the un-entangled regime and in which the wall-to-wall distance between fillers is on the order of the chain size. Although conceptually simple, the model captures the main features that distinguish nanocomposite and microcomposite behaviors, for example, the rubber-like response at low frequencies and the enhanced reinforcement at low deformation rates. Therein, since the fillers are sufficiently close to each other, polymeric chains act as bridges and form a network akin to the situation in rubbers. The dynamics of this network is controlled by the dynamics of the process of attachment/detachment of chains to/from fillers.

In this article,we consider the cases of concentrated entangled polymeric liquids that interact strongly with filler particles. The fillers are assumed to be rigid and spherical, and to be homogeneously dispersed in the matrix (non-agglomerated). The structure of this system was studied by Ozmusul et al. (2005), by means of molecular computer simulation.

The effect of entanglements on the filled polymer dynamics is captured by using the Generalized Rouse Model (GRM). In this framework, the interaction of the representative chain with its neighbors is purely frictional, similar to the original Rouse model (Kavassalis and Noolandi 1987, 1988). However, the presence of entanglements destroys the three-dimensional isotropy of polymer diffusional motion leading to non-equivalent longitudinal and transverse modes. The confinement is represented by using different friction coefficients for the longitudinal and transverse relaxation modes. The influence of the filler-polymer interaction (attachment/detachment kinetics) is captured within a continuum approximation: an attachment point is represented as a region of enhanced friction for the respective chain. A similar approach was used to model the boundary layer friction of confined polymer melts (Subbotin et al. 1997). Hence, the fillers are not represented explicitly in the model, rather their effect is framed in a manner consistent with the GRM.

Since we put the topological and energetic constrains to chain motion in a unified framework, that of *friction laws*, here it is further possible to capture polymer viscoelastic nonlinearities such as the convectional constraint release (Marrucci 1996). One of the objectives of this work is to examine the extent to which such a formulation based on the law of friction may describe the viscoelasticity of filled melts and concentrated polymer solutions.

This study is organized as follows. We first examine the diffusion equation for a bead-spring model of an adsorbed chain with anisotropic friction. The full solution is sought for the simplified case of a nonlinear dumbbell with single relaxation time. The effect of the various model parameters is studied on particular types of flow, and the model is compared with experimental data. The paper concludes with a summary and discussion of possible future extensions.

Generalized bead-spring model for the nano-composite

We consider a system of linear monodisperse amorphous homopolymers and a random distribution of non-aggregated rigid spherical nanoparticles. The fillers are uniformly distributed in 3D. An average chain conformation is schematically depicted in Fig. 1. The dispersed particles are sufficiently small such that even at low volume fractions, the average particle wall-to-wall distance is on the order of the size of the average polymer coil. Hence, in equilibrium, any chain may simultaneously attach to one or more nanoparticles. Each adsorbed polymer chain section includes a succession of polydisperse loops and train segments (Ozmusul et al. 2005). In addition, there exists a large number of polydisperse dangling tails in the matrix (segments connected at one end to the filler and having the other end free).

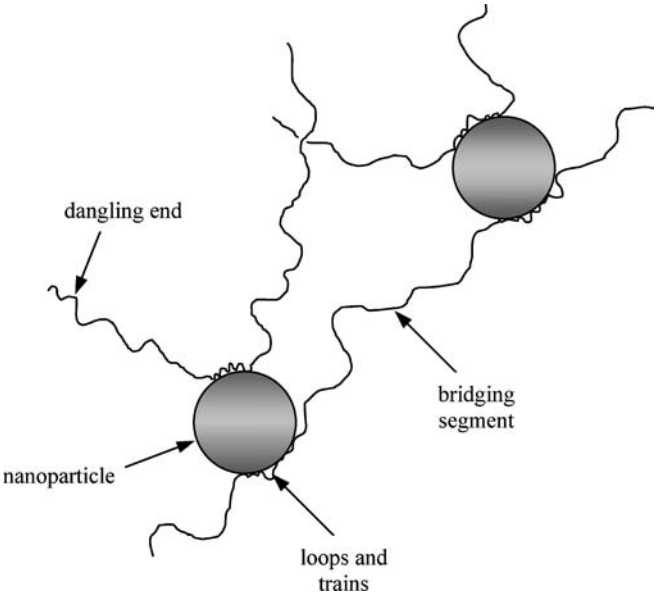

Fig. 1 Schematic representation of adsorbed representative chains

As in the Doi–Edwards reptation theory (1986), the representative chain is assumed to be "confined" by a "tube" representing topological constraints to its motion. In the reptation theory, the diameter of this tube represents the average distance between entanglements. Here, we apply the idea of anisotropic effects to the simpler kinetic theories (Deaguiar 1983; Bird and Wiest 1984). Bird and Deaguiar (1983) introduced the encapsulated dumbbell model, in which the Brownian motion and hydrodynamic drag acting on each bead are not isotropic. In their model, the dumbbell is constrained to move within a "capsule" region due to the lateral topological constraints. This idea was also advanced in the more general case of multi-bead chains by Curtiss and Bird (1981) as an alternative to the reptation theory. The similarity between these approaches and the reptation theory was studied by Baxandall (1987), who showed that the reptation picture emerges by postulating anisotropic hydrodynamic forces,without recourse to the anisotropic Brownian motion.

The polymeric chains are represented here as freely joined bead-springs subjected to anisotropic friction (with non-bonded neighbors) and connected (with some probability) to fillers. Each coarse grained chain consists of M beads which are connected by $M-1$ springs. The vector $\mathbf{r}_i$ represents the position of the ith bead, while $\mathbf{R}_i = \mathbf{r}_{i+1} - r_i$ is the connector vector.

The configurational distribution function for the representative chain, ψ ($\mathbf{R}_1$, $\mathbf{R}_2$, ..., $\mathbf{R}_{M-1}$, t), satisfies the following continuity equation (Bird et al. 1987):

$$\frac{\partial \psi}{\partial t} = -\sum_{i=1}^{M-1} \frac{\partial}{\partial \mathbf{R}_i} \cdot (\dot{\mathbf{R}}_i \psi). \tag{1}$$

As in the classical Rouse model, the evolution equations for $\dot{\mathbf{R}}_i$ are obtained from the total force balance (equation of motion) of each bead. Neglecting the inertia term, these read

$$\mathbf{F}_i^{(e)} + \mathbf{F}_i^{(Br)} + \mathbf{F}_i^{(h)} = 0, \quad i = 1, 2, \ldots M. \tag{2}$$

The three terms in Eq. 2 represent the effect of entropic, Brownian, and hydrodynamic forces, respectively. The entropic spring force is given by

$$\mathbf{F}_i^{(e)} = \sum_{k=1}^{M-1} (\delta_{ki} - \delta_{k+1i}) F_k^{(c)} \frac{\mathbf{R}_k}{R_k}, \tag{3}$$

where $F_k^{(c)}$ is the modulus of the connector force between adjacent beads, defined by $\mathbf{F}_k^{(c)} = -\nabla U_{\mathrm{el}}(\mathbf{R}_k)$. Here, U_{el} represents the entropy-controlled elastic free energy between beads.

The velocity distribution is assumed to be Maxvellian and thus, the time average of fluctuating Brownian force on the ith bead reads

$$\mathbf{F}_i^{(B)} = -k_{\mathrm{B}} T \frac{\partial}{\partial \mathbf{r}_i} \ln \psi. \tag{4}$$

The hydrodynamic force may be calculated using an anisotropic Stock's law as

$$\mathbf{F}_i^{(h)} = -\xi_i . (\dot{\mathbf{r}}_i - \kappa . \mathbf{r}_i). \tag{5}$$

Here, $\xi_i = k_{\mathrm{B}} T \mathbf{D}_i^{-1}$ is the tensorial friction coefficient and $\mathbf{D}_i$ is the diffusion tensor. The convective motion of the beads in the flow is characterized by the macroscopic velocity gradient tensor κ.

In order to represent the confinement of the chain motion within its tube, the diffusional motion is decomposed in the direction along and perpendicular to the tube axis. The friction coefficient in Eq. 5 is taken to be anisotropic

$$\xi_i = (\xi_l)_i \mathbf{u}_i \mathbf{u}_i + (\xi_t)_i (\mathbf{I} - \mathbf{u}_i \mathbf{u}_i), \tag{6}$$

where $\mathbf{u}_i$ is a unit vector along $\mathbf{R}_i$ and $\mathbf{I}$ is identity tensor. In theory, the corresponding values of the longitudinal and transverse friction coefficients (ξ_l and ξ_t, respectively) depend on the diameter of the encompassing tube (on the order of the entanglement distance) in the coarse grained model compared with the bead size (on the order of the Kuhn segment length). If the bead size is similar with the average tube diameter (i.e., highly entangled systems), the lateral diffusion of the bead is retarded due to the presence of topological constrains, and hence, in states close to equilibrium one may take $\xi_t \gg \xi_l$ (Kavassalis and Noolandi 1988). In this work, the effect of attachment to fillers on dynamics is also captured by means of these friction coefficients. An attachment point is represented as a region of the chain in which the friction is more pronounced.

The material internal structure is subjected to change after the inception of macroscopic flow. This deviation from the equilibrium configuration, which is accompanied by the emergence of nonlinear viscoelasticity, is the result of topological constraint release as well as the promotion of chain detachment from filler surfaces (energetic stick-slip process). Inspired by the theory of convectional constraint release (Marrucci 1996; Marrucci and Ianniruberto 1997) for both modes of motion (longitudinal and transverse), the friction coefficient ξ associated with the diffusion of each bead is decomposed into the sum of a topological term ξ_{top}, which is influenced by flow and possibly vanishes at high deformation rates, and a constant irreducible term ξ_{irr}, which accounts for self diffusion and is independent of topology.

More precisely, for the longitudinal motion of an adsorbed bead, we have

$$(\xi_l)_i = (\xi_{\mathrm{ad}})_i + \xi_0, \tag{7}$$

where ξ_0 is the friction coefficient corresponding to self diffusion of a single bead and accounts for its friction with the solvent molecules and/or other non-bonded polymer beads. Using a simple activation model (Frenkel 1946) for a bead of size l, this friction coefficient is approximated by $\xi_0 = 2k_B T\tau_0 / l^2$, with the time constant τ_0 being

$$\tau_0 = \tau^* \exp\left(\frac{U_0}{k_B T}\right). \tag{8}$$

Here $\tau^* \sim l\sqrt{m/k_B T}$ is the characteristic time of molecular vibrations, and U_0 is the activation energy for diffusion of a segment in the bulk, and m is its mass.

The first term in Eq. 7, ξ_{ad}, represents the increase in longitudinal friction due to the polymer-filler contact points. This term may be evaluated by a similar thermal activation model (Subbotin et al. 1997). The additional friction due to the attachment is given by $\xi_{ad} = 2k_B T\tau_{ad}/l^2$, where the effective time constant of detachment, τ_{ad}, is defined as

$$\tau_{ad} = \tau^* \exp\left(\frac{U_{ad} - F_i^{(e)}\delta}{k_B T}\right). \tag{9}$$

Here $\tau^* \sim l\sqrt{m/k_B T}$ is the inverse of the detachment attempt frequency, as before, and U_{ad} is the adsorption energy to the filler surface. This last quantity is evaluated as the energy difference of a bead residing on a filler surface and its energy in the bulk. In Eq. 9 it is acknowledged that the detachment process is favored by the tension $F^{(e)}{}_i$ exerted on the adsorbed bead by the adjacent strand(s) (Fig. 2). δ is a constant activation length.

The friction coefficient for the transverse mode is expressed as

$$(\xi_t)_i = (\xi_l)_i + \frac{1}{(\xi_{en})_i^{-1} + \alpha_i \left|\kappa{:}\langle \mathbf{R}_i \mathbf{R}_i\rangle - \frac{1}{2}\frac{d}{dt}\langle R_i^2\rangle\right|}, \tag{10}$$

where $\langle ... \rangle$ denotes $\int \ldots \psi\ (\mathbf{R})\, d\mathbf{R}$ representing the ensemble average of the respective quantity and α_i is a positive constant. The transverse friction coefficient is always larger than the longitudinal coefficient. $(\xi_{en})_i$ represents friction associated with the lateral constraint on a single bead (entanglements). The second term in the denominator of the right hand side of Eq. 10 stands for the renewal of topological constrains through the relative motion of chains during flow and is similar to that used by Marrucci (1996) to represent constraint release. The constraint release here affects the chain motion in the transverse direction only, i.e. those constraints that prevent the Rouse relaxation of the tube. The two limits of Eq. 10 are: under equilibrium it reduces to

$$(\xi_t)_i = (\xi_{ad})_i + \xi_0 + (\xi_{en})_i, \tag{11}$$

while under the effect of fast flows and intense constraint release it becomes

$$(\xi_l)_i \approx (\xi_t)_i. \tag{12}$$

Equations 3, 4 and 5 for the forces acting on each bead are substituted in Eq. 2, which is then solved for $\dot{\mathbf{R}}_i$. Then, the diffusion Eq. 1 becomes

$$\frac{\partial \psi}{\partial t} = -\sum_{i=1}^{M-1} \frac{\partial}{\partial \mathbf{R}_i} \cdot \left(\kappa.\mathbf{R}_i \psi - \sum_{j=1}^{M-1} \mathbf{D}_{ij}.\left[\frac{\partial \psi}{\partial \mathbf{R}_j} + \frac{1}{k_B T}\mathbf{F}_j^{(e)}\psi\right]\right), \tag{13}$$

where

$$\mathbf{D}_{ij} = k_B T[(\xi_i^{-1} + \xi_{i+1}^{-1})\delta_{ji} - \xi_{i+1}^{-1}\delta_{ji+1} - \xi_i^{-1}\delta_{j+1i}]. \tag{14}$$

Finally, stress production is evaluated based on entropic interactions only. The stress is expressed using the virial formula (Kramers' expression) as

$$\tau = -\rho\left\langle \sum_{i=1}^{M-1} \mathbf{F}_i^{(e)}\mathbf{R}_i \right\rangle + \rho(M-1)k_B T\mathbf{I}, \tag{15}$$

where ρ is the chain number density, and the angular parentheses represent ensemble average.

Reduction to a dumbbell model

In order to predict the constitutive response of the material, Eq. 13 must be integrated for the time

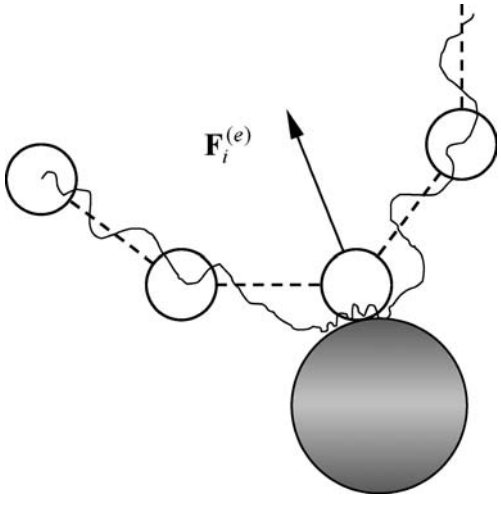

Fig. 2 The ith adsorbed bead is pulled from the filler surface by the entropic force in the adjacent strands. The actual chain is shown with continuous line, along with the corresponding bead-spring schematic. The force represents the net effect of the two strands adjacent to the attached bead

evolution of the distribution function, ψ. The stress is computed from Eq. 15 using ψ.

Two simplifying assumptions are necessary before the solution of Eq. 13 is attempted. First, it is assumed that the probability of bead-filler attachment is constant along the chain. Therefore, the representative chain has constant friction ξ_{ad} along its contour, i.e. $(\xi_{ad})_i = \xi_{ad}$. This is a mean field-type approximation for the effect of fillers on chain mobility. Furthermore, it is assumed that all friction coefficients are constants in time and during deformation. Second, in order to render Eq. 13 tractable, each molecule is regarded as and encapsulated elastic dumbbell with single relaxation time (Bird and Deaguiar 1983) (Fig. 3). The dumbbells are composed of two beads connected by an entropic spring.

The dumbbell model is obtained by preserving only one term in the right hand side of Eq. 13 ($M = 2$); i.e.,

$$\frac{\partial \psi}{\partial t} = -\nabla \cdot \left(\kappa . \mathbf{R} \psi - \mathbf{D} . \left[\nabla \psi + \frac{1}{k_B T} \mathbf{F}^{(e)} \psi \right] \right). \tag{16}$$

Here, the diffusion tensor $\mathbf{D}$ reads

$$\mathbf{D} = 2 k_B T \xi^{-1} = D_l \mathbf{uu} + D_t (\mathbf{I} - \mathbf{uu}), \tag{17}$$

and $\mathbf{u}$ shows the unit vector parallel with the dumbbell's end to end vector $\mathbf{R}$. Following Marrucci and Ianniruberto (2001) we pre-average the tensor $\mathbf{D}$ simply by replacing $\mathbf{uu}$ with the ensemble average $\langle \mathbf{uu} \rangle$, which itself is approximated by the ratio $\langle \mathbf{RR} \rangle / \langle R^2 \rangle$. Hence, the diffusion tensor $\mathbf{D}$ can be written as

$$\mathbf{D} = D_l \left(\beta \mathbf{I} + (1 - \beta) \frac{\langle \mathbf{RR} \rangle}{\langle R^2 \rangle} \right). \tag{18}$$

where $\beta = D_t / D_l$.

Using Eqs. 7, 10, the conformational-dependent diffusion coefficients are defined as

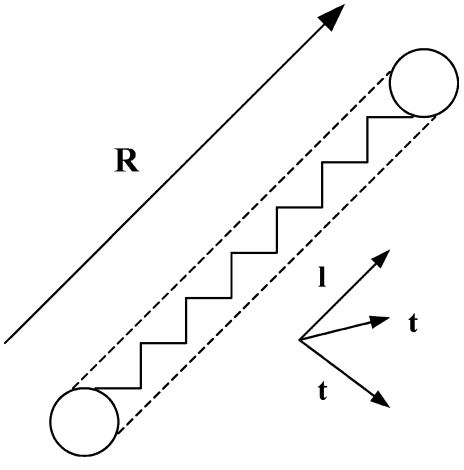

Fig. 3 The adsorbed "encapsulated" FENE dumbbell with anisotropic friction, where $\xi_t > \xi_l$

$$\frac{1}{D_l} = \frac{1}{D_{ad}} + \frac{1}{D_0}, \tag{19}$$

$$\frac{1}{D_t} = \frac{1}{D_l} + \frac{1}{D^0_{en} + D^c_{en}}. \tag{20}$$

where D_0 stands for the irreducible self-diffusion coefficient of each dumbbell bead, given by $(2k_B T)/(N\xi_0)$, with N being the total number of statistical segments in the original macromolecule. D_{ad} and $D^0{}_{en}$ represent the effect of energetic polymer-particle interactions and equilibrium topological polymer-polymer entanglement constraints, respectively, on the dumbbell diffusional motion. D^c_{en} is the corresponding mean-field diffusion coefficients due to convective constraint release. These quantities are given by

$$D_{ad} = \frac{2 k_B T}{c N \xi_{ad}}, \tag{21}$$

$$D^0_{en} = \frac{2 k_B T}{N \xi_{en}}, \tag{22}$$

$$D^c_{en} = \alpha \left| \kappa : \langle \mathbf{RR} \rangle - \frac{1}{2} \frac{\mathrm{d}}{\mathrm{d}t} \langle R^2 \rangle \right|. \tag{23}$$

Here, c is the fraction of the representative chain segments adsorbed to fillers in the equilibrium configuration, and α is a positive constant. To the best of authors' knowledge, other than the scaling description for polymer adsorption on a *single* colloidal particle by Aubouy and Raphaël (1998), there is no analytical method to estimate the value of c, especially for the case of multiparticle structures. This information can be obtained from molecular simulations of the equilibrium structure. Such simulations have been performed for various filler wall-to-wall distances and various levels of the energetic interaction between polymers and fillers (Ozmusul et al. 2005). The main conclusions from that study are also summarized by Sarvestani and Picu (2004).

Multiplying both sides of Eq. 16 by $\mathbf{RR}$, an evolution equation for the second moment of the distribution function results

$$\frac{\mathrm{d}}{\mathrm{d}t} \langle \mathbf{RR} \rangle = \kappa . \langle \mathbf{RR} \rangle + \langle \mathbf{RR} \rangle . \kappa^{\mathrm{T}} + 2\mathbf{D} - \frac{3}{R^2_0} (\mathbf{D} \cdot \langle \mathbf{RR} \rangle + \langle \mathbf{RR} \rangle \cdot \mathbf{D}), \tag{24}$$

where $R^2{}_0$ is the mean square length of the end-to-end vector of the equilibrium chains. To obtain Eq. 24, the dumbbells are assumed Hookean and the entropic force is taken as $\mathbf{F}^{(e)} = (3k_B T / R^2{}_0)\mathbf{R}$.

Taking trace of Eq. 24 we obtain

$$\kappa : \langle \mathbf{RR} \rangle - \frac{1}{2} \frac{\mathrm{d}}{\mathrm{d}t} \langle R^2 \rangle = p D_l, \tag{25}$$

where

$$p = \frac{3}{R_0^2}\left(\frac{1-\beta}{\langle R^2\rangle}\langle \mathbf{RR}\rangle{:}\langle \mathbf{RR}\rangle + \beta\langle R^2\rangle\right) - (2\beta+1). \quad (26)$$

Substituting Eqs. 25, 26 into Eq. 20 yields the following expression for the transverse mode of motion:

$$D_t = \left(\frac{1}{D_l} + \frac{1}{D_{\mathrm{en}}^0 + \alpha|p|D_l}\right)^{-1} \quad (27)$$

Therefore, the time evolution of $\mathbf{A} = \langle \mathbf{RR}\ \rangle$, the second moment of the distribution function of the end-to-end vector, may be obtained as

$$\frac{\mathrm{d}}{\mathrm{d}t}\mathbf{A} = \kappa.\mathbf{A} + \mathbf{A}.\kappa^{\mathrm{T}} + 2D_l\left(\beta\mathbf{I} + (1-\beta)\frac{\mathbf{A}}{Tr\mathbf{A}}\right) - \frac{6D_l}{R_0^2}\left(\frac{1-\beta}{Tr\mathbf{A}}\mathbf{A}.\mathbf{A} + \beta\mathbf{A}\right). \quad (28)$$

Eq. 28 may be solved, in principle, for any flow regime. In the next section we present its solution for the 2D Couette flow. Under this condition, the shear stress driving the flow can be expressed as

$$\tau_{12} = \frac{3\rho k_{\mathrm{B}}T}{R_0^2}A_{12}, \quad (29)$$

In steady-state flows, all time derivatives in Eq. 28 vanish and the system reduces to a set of algebraic nonlinear equations.

Results and comparison with experiments

In this section, we qualitatively examine the steady state response of nanofilled polymer composites subjected to 2D shear flow and then quantitatively compare the predictions of the model with relevant experimental observations.

Effect of model parameters

We begin by studying the qualitative behavior of the model. For this purpose, we take R_0 as the unit of length, while the unit of time is $\tau = (R^2{}_0/6D_0)$. The activation length δ is assumed to be on the order of $\approx R_0/10$. Two non-dimensional quantities prove useful in numerical studies:

$$\varepsilon = \exp\left(\frac{U_{\mathrm{ad}} - U_0}{k_{\mathrm{B}}T}\right) \quad \varepsilon' = \frac{\xi_{\mathrm{en}}}{\xi_0}, \quad (30)$$

where the former represents the relative polymer-filler affinity (energetic), while the latter represents the anisotropy in diffusion of the representative bead in the longitudinal and transverse tube directions, i.e. the degree of entanglement. Note that in non-entangled systems $\varepsilon' = 0$. Positive values represent various degrees of confinement of the representative chain to the tube, with ε' being in principle dependent on the tube diameter. It is also assumed that in Eq. 22 $\alpha = 0.5$ (Marrucci 1996).

Figure 4 shows the variation of the steady-state shear viscosity (η) of the reinforced polymer with the applied shear rate ($\dot{\gamma}$). Here, we assume $\varepsilon = 10{,}000$ and $\varepsilon' = 1$ (moderately entangled systems). As mentioned earlier, c is the fraction of adsorbed statistical segments of the representative chain in the unloaded, equilibrium state. This parameter is approximately proportional to the filler-matrix interfacial area. For a ratio of attached segments, c, as low as 0.1%, the magnitude of the zero shear viscosity dramatically increases compared to the viscosity of the neat polymer. A similar trend is observed in experiments even at very low concentration of well-dispersed nanoparticles (Zhang and Archer 2004). This is in marked contrast with the predictions based on continuum viscoelasticity (e.g. the Einstein relation for colloidal suspensions). In the present model, this behavior is solely due to the energetic interactions between polymer chains and fillers. The increase of c leads to an almost proportional increase of the zero shear rate viscosity.

Shear thinning becomes more pronounced as the filler concentration (and the average number of chain-filler attachments) increases. Shear thinning in the neat polymer is due to the convective constraint release at high strain rates. The amount of thinning in the filled polymer under steady-state conditions increases due to the additional effect of chain-filler detachment. At low strain rates, the processes of detachment and chain-filler re-attachment balance each other and we conjecture that

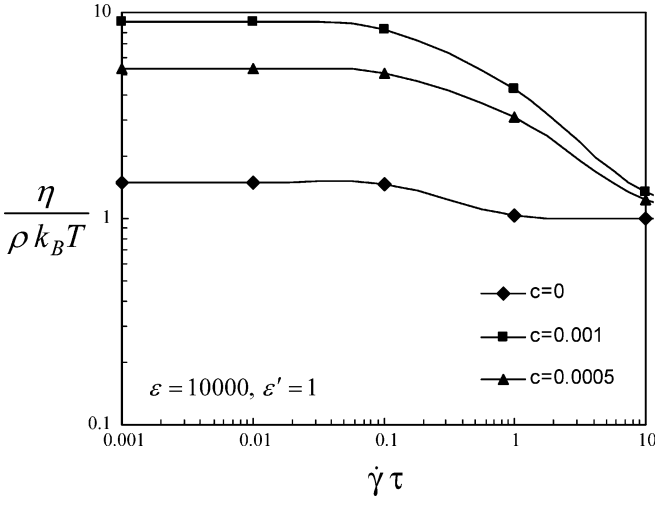

Fig. 4 Variation of the steady-state normalized shear viscosity with the shear rate for three values of the polymer-filler attachment fraction c

the re-attached chains have equilibrium conformations on the re-attachment time scale. Hence, the equilibrium structure and zero strain rate material response are recovered. The detachment process contributes a fraction of the flow stress and rate sensitivity. At high rates, the detachment is more pronounced than re-attachment, which leads to a reduction in flow stress and shear thinning. Moreover, the onset of shear thinning shifts towards the lower shear rates as the ratio of adsorbed segments increases, indicating the increase in chain relaxation time.

In order to study the model prediction of molecular birefringence, we compute the orientation component A_{12} and the alignment angle $\chi = (1/2)\ \tan^{-1}(2A_{12}/A_{11} - A_{22})$ at various shear rates. These quantities are shown in Figs. 5a, b, respectively. A_{12} is directly proportional to the index of refraction and to the output of birefringence measurements. Deformation produces chain alignment, with the effect being more pronounced as the rate increases. At very large rates, larger than the dominant relaxation rate, saturation is seen in both the model and experiments. As shown in the two figures, chain alignment is enhanced by the presence of fillers and the effect increases with c. This is expected as the frictional effect of fillers slows down chain relaxation. The onset of saturation (non-linear behavior of the birefringence versus strain rate) in Fig. 5a depends on filler concentration, with the effect being observed at lower strain rates as c increases. Furthermore, all curves seem to eventually converge at the same saturation plateau. In the model, this is due to the fact that at high strain rates the rate of chain detachment from fillers is larger than that of re-attachment, and hence, the neat polymer limit is recovered. This is only an approximation since we neglect the effect of the excluded volume of fillers on the rheology here.

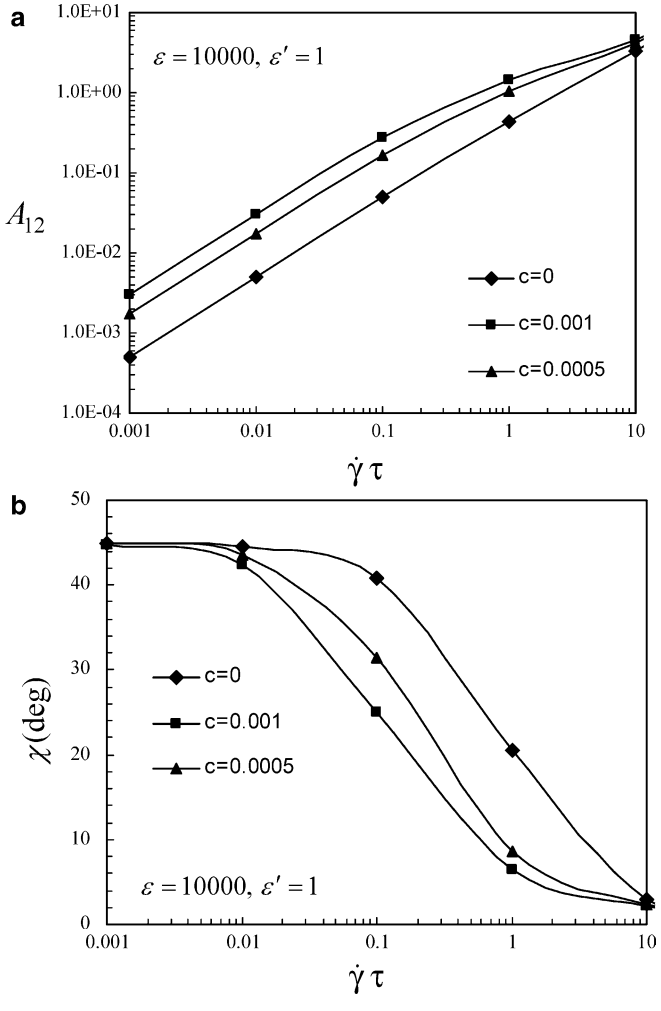

Fig. 5 Variation of the steady-state values of the **a** orientation component A_{12} and **b** alignment angle χ with shear rate, for various polymer-filler attachment fractions c

In Fig. 6, we show the sensitivity of viscosity to the affinity parameter ε for $\varepsilon' = 1$ and $c = 0.001$. The results are shown at three different shear rates. The graphs clearly illustrate the crucial importance of the polymer-particle affinity for the rheological response of the system. It is interesting to observe that in the present case, since we neglect the excluded volume of fillers, they do not affect the rheology as long as the affinity parameter ε is smaller than 100. This provides an indication as to what type of surface treatment is required in a certain system in order for the filling to be effective. At higher affinities, the viscosity increases non-linearly with ε.

Comparison with experimental results

Next, a quantitative comparison is made with the experimental data reported by Zhang and Archer (2004).

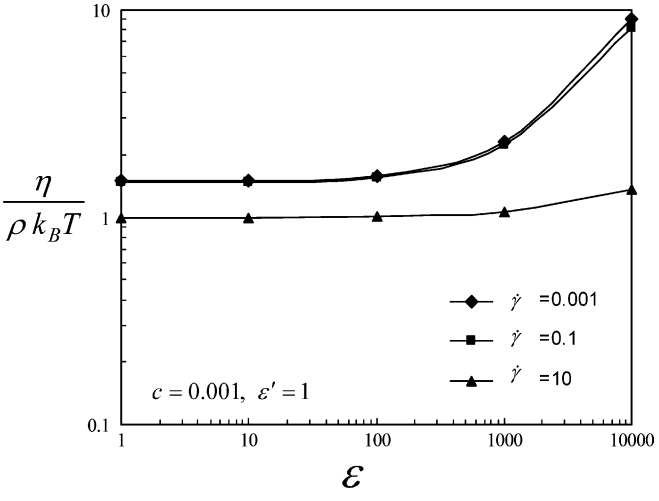

Fig. 6 Effect of the affinity parameter ε on the viscosity at three different shear rates

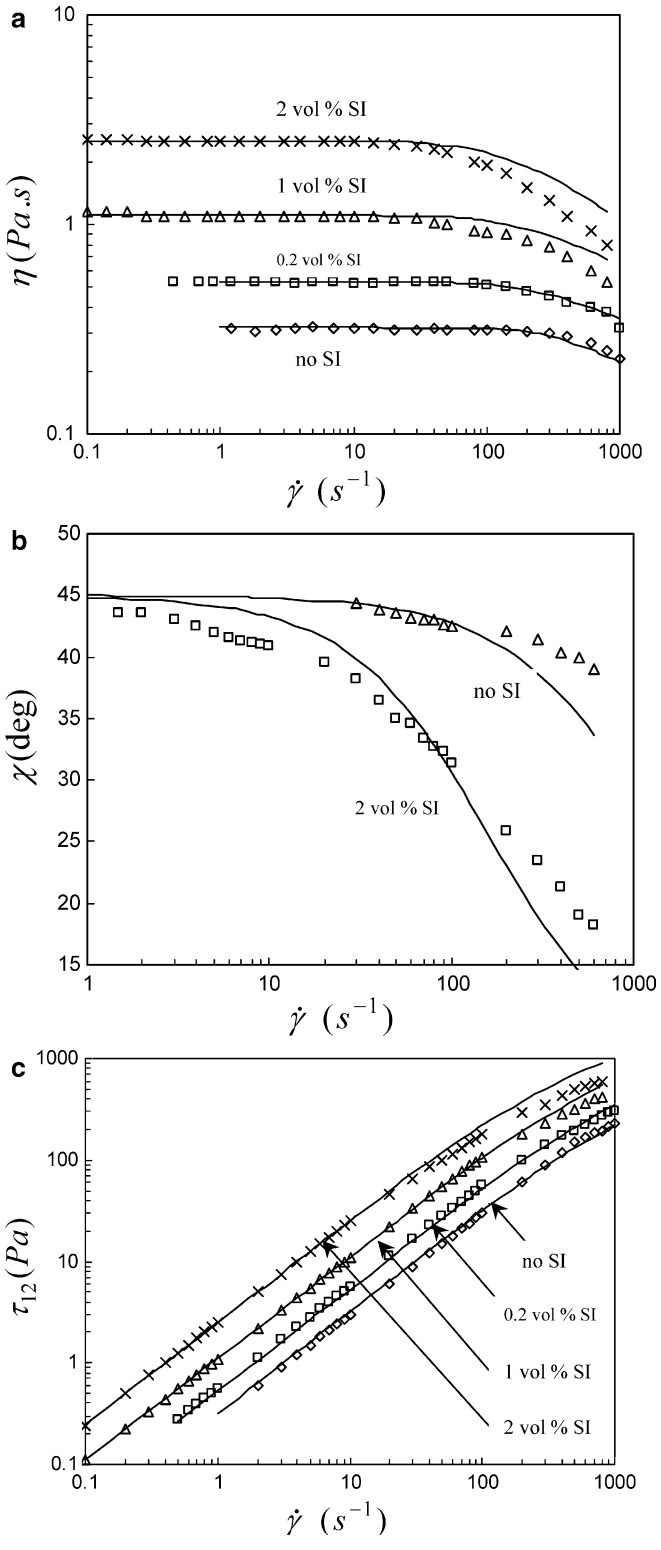

Fig. 7 Comparison of calculated **a** viscosity, **b** alignment angle, and **c** shear stress with equivalent experimental data of Zhang and Archer (2004). Predictions for the neat polymer are obtained by using $\xi_0 = 2.3 \times 10^{-12}$ kg/s, and $\varepsilon' = 0.66$. For filled systems, the curves result by taking $c\xi_{ad}$ equal to 1.05, 4.0, and 11.3, for 0.2%, 1%, and 2% filler volume fraction, respectively

They investigated the rheology of semidilute aqueous solutions of poly(ethylene oxide) (PEO) containing a homogeneous dispersion of nanosized silica particles. We use data for 4.6 wt % of linear PEO at 25°C. The polymers have narrow molecular weight distribution ($\bar{M}_w/\bar{M}_n = 1.06$) with $\bar{M}_w = 700,000$ g/mol. Spherical silica particles have narrow size distribution with an average diameter of $\sim$ 12 nm. In the experiment, the silica particles were surface modified by grafting 2-[methoxy(polyethyleneoxy)propyl] trimethoxysilane.

The chain length is evaluated as $N \sim \bar{M}_w/137$ and the Kuhn segment length is 1.1 nm (Rubinstein and Colby 2003). The average length of the end-to-end vector of a representative PEO chain results 88 nm. The average wall-to-wall distance at this filler volume fraction (2 vol%) is 59 nm. Hence, the average wall-wall distance is between R_g and $2R_g$. Using scaling relations for semidilute solutions, it is possible to infer that the given polymer concentration (4.6 wt %) is above coil overlapping and entanglement thresholds (Rubinstein and Colby 2003).

The values of the friction parameters ξ_0 and ε' are determined by fitting the model to the experimental data for the neat polymer. Since the experiments are performed at relatively small strain rates at which the nonlinear behavior is not fully manifest, we disregard the contribution of convective constraint release. We find $\xi_0 = 2.3 \times 10^{-12}$ kg/s, and $\varepsilon' = 0.66$. Based on this, the longest relaxation time of the system is expected to be on the order of 1 μs, which is in agreement with experimental measurement of Zhang and Archer (2004).

The adsorption energy of PEO to the surface treated silica particles is unknown and hence, we cannot predetermine the value of U_{ad}. Instead, we extract the parameter $c\xi_{ad}$ from the Newtonian part of log η versus log $\dot{\gamma}$ of filled samples. Finally, the activation length δ is determined by fitting the onset of the non-linear regime for one of the filled polymer curves. The activation length results equal to almost five Kuhn segments.

The model prediction for viscosity η, alignment angle χ, and shear stress τ_{12} are evaluated using these parameters and are compared with the experimental data in Fig. 7a–c. The degree of agreement is encouraging considering the simplicity of the model. Some disagreement is seen at higher filler volume fraction in the non-linear range. It appears that the dumbbell approximation is too crude to capture the details of the stick-slip process on filler surfaces involving polydisperse trains and loops. However, the model predictions do follow the stress-optical rule, as expected.

The linear viscoelastic response of the system can also be predicted using the present model. In the low frequency region, the slopes of both storage and loss

moduli increase with c from the values corresponding to the unfilled material. However, no terminal plateau is obtained when the wall-wall distance is on the order of R_g. This effect, which is observed in experiments and is captured by our network model (Sarvestani and Picu 2004), is assumed to be due to the presence of short polydisperse bridging segments between neighboring fillers. While the network model effectively captures this behavior, the present frictional model does it only approximately.

Zhang and Archer (2004) also report the stress optical coefficient. They observed that, at low rates, the dispersion of nanofillers into the polymer leads to larger stress optical coefficients compared to the neat polymer solution. This is due to the enhanced stress production in the filled system associated with the formation of the secondary network of polymer bridging chains between fillers. At high deformation rates, however, the SOC of the filled material converges to that of the unfilled system. This violation of the stress optical rule is attributed to the formation of mesoscale structures of filler agglomerates and to the orientation/deformation of these clusters during flow. This larger scale effect is not considered in the present model.

Conclusions

A model for filled concentrated solutions and polymeric melts is proposed. The focus is on systems with small fillers, in which the filler wall-to-wall distance is on the order of the chain gyration radius and in which the energetic interaction of polymers and fillers is strong. In such systems, every chain has an equal chance to be adsorbed on the fillers. The main focus here is on capturing two major effects: entanglements and the process of attachment/detachment of chains from fillers. These are assumed to play the most prominent role in the rheology of these materials. The dynamics is modeled using classical concepts of polymer physics: the entanglements are modeled using the Generalized Rouse Model, while the stick-slip process of the chain-filler interaction is modeled in a homogenized way through an additional friction force. Hence, the model is purely frictional in nature.

The sensitivity of the model to the various parameters is studied. Their values are obtained by fitting the mechanical response of the neat polymer (for parameters representing entanglements) and the zero shear rate viscosity of one filled system (for parameters describing the chain-filler attachment/detachment process). The model predictions are compared with experimental data. The agreement is good, although some discrepancies exist in the highly non-linear range of strain rates.

The advantage of the model derives from its simplicity and conceptual unity. The parameters are easy to fit to experimental data and have transparent physical meaning. Its drawbacks and limitations are related to the homogenized representation of the polymer-filler attachments and the dumbbell simplification used in the solution.

References

Aubouy M, Raphaël E (1998) Scaling description of a colloidal particle clothed with polymers. Macromolecules 31:4357–4363

Baxandall LG (1987) Anisotropic friction in polymer models. I. The elastic dumbbell and reptating chain. J Chem Phys 87:2297–2304

Bird RB, Deaguiar JR (1983) An encapsulated dumbbell model for concentrated polymer solutions and melts I. Theoretical development and constitutive equation. J Non-Newtonian Fluid Mech 13:149–160

Bird RB, Wiest JM (1984) Anisotropic effects in dumbbell kinetic theory. J Rheol 29:519–532

Bird RB, Armstrong RC, Hassager O (1987) Dynamics of polymeric liquids, vol 2. Wiley, New York

Cassagnau Ph, Mélis F (2003) Non-linear viscoelastic behavior and modulus recovery in silica filled polymers. Polymer 44:6607–6615

Curtiss CF, Bird RB (1981) A kinetic theory for polymer melts. I. The equation for the single-link orientational distribution function. J Chem Phys 74:2016–2025

Deaguiar JR (1983) An encapsulated dumbbell model for concentrated polymer solutions and melts II. Calculation of material functions and experimental comparisons. J Non-Newtonian Fluid Mech 13:161–179

Doi M, Edwards SF (1986) Theory of polymer dynamics. Clarendon, Oxford

Donnet JB (2003) Nano and microcomposites of polymers elastomers and their reinforcement. Compo Sci Technol 63:1085–1088

Frenkel J (1946) Kinetic theory of liquids. Clarendon, Oxford

Havet G, Isayev AI (2001) A thermodynamic approach to the rheology of highly interactive filler-polymer mixtures: Part I-Theory. Rheol Acta 40:570–581

Havet G, Isayev AI (2003) A thermodynamic approach to the rheology of highly interactive filler-polymer mixtures. Part II-Comparison with polystyrene/nanosilica mixtures. Rheol Acta 42:47–55

Heinrich G, Klüppel M (2002) Recent advances in the theory of filler networking in elastomers. Adv Polym Sci 160:1–44

Kavassalis TA, Noolandi J (1987) New view of entanglements in dense polymer systems. Phys Rev Lett 59:2674–2677

Kavassalis TA, Noolandi J (1988) A new theory of entanglements and dynamics in dense polymer systems. Macromolecules 21:2869–2879

Leonov AI (1990) On the rheology of filled polymers. J Rheol 34:1039–1068
Marrucci G (1996) Dynamics of entanglements: a nonlinear model consistent with the Cox-Merz rule. J Non-Newtonian Fluid Mech 62:279–289
Marrucci G, Ianniruberto G (1997) Effect of flow on topological interactions in polymers. Macromol Symp 117:233–240
Marrucci G, Ianniruberto G (2001) Constitutive equation for polymeric solution close to the overlap concentration. Chem Eng Sci 56:5539–5544
Ozmusul MS, Picu RC, Sternstein SS, Kumar S (2005) Lattice Monte Carlo simulations of chain conformations in polymer nanocomposites. Macromolecules (in press)
Reynaud E, Jouen T, Gauthier C, Vigier G, Varlet J (2001) Nanofillers in polymeric matrix: a study on silica reinforced PA6. Polymer 42:8759–8768
Rubinstein M, Colby RH (2003) Polymer Physics. Oxford University Press, London
Sarvestani AS, Picu RC (2004) Network model for viscoelastic behavior of polymer nanocomposites. Polymer 45:7779–7790
Subbotin A, Semenov A, Manias E, Hadziioannou G, ten Brinke G (1995) Rheology of confined polymer melts under shear flow: strong adsorption limit. Macromolecules 28:1511–1515
Subbotin A, Semenov A, Doi M (1997) Friction in strongly confined polymer melts: effect of polymer bridges. Phys Rev E 56:623–630
Zhang Q, Archer LA (2002) Poly(ethylene oxide)/silica nanocomposites: structure and rheology. Langmuir 18:10435–10442
Zhang Q, Archer LA (2004) Optical polarimetry and mechanical rheometry of poly(ethylene oxide)-silica dispersions. Macromolecules 37:1928–1936